Cellulose (2021) 28:5477–5492
https://doi.org/10.1007/s10570-021-03866-y

ORIGINAL RESEARCH

Characterization of natural cellulosic fibers from *Yucca aloifolia* L. leaf as potential reinforcement of polymer composites

Hederson Majela do Nascimento · Andressa dos Santos · Vitor Anthony Duarte · Paulo Rodrigo Stival Bittencourt · Eduardo Radovanovic · Silvia Luciana Fávaro

Received: 9 July 2020 / Accepted: 30 March 2021 / Published online: 6 May 2021

Abstract In this work lignocellulosic fibers were obtained from *Yucca aloifolia* L. leaves and their chemical, morphological, thermal and mechanical properties were studied. The fibers were pullout from the leaves and characterized by infrared spectroscopy (ATR-FTIR), X-ray diffraction (XRD), chemical characterization, thermogravimetric analysis (TGA), single fiber tensile tests and scanning electron microscopy (SEM). The cellulose crystallinity index found was 69.43%. The fibers presented a high cellulose content, ~ 52.5%, and they are thermally stable until 193.4 °C. The tensile test for single fibers showed average results for the tensile strength of 800 MPa, Young's modulus of 39 GPa, and 2% strain at failure. Morphological analysis indicated the presence of a large number of parenchymal cells and not cellulosic constituents in fiber surface. These results indicated that *Yucca aloifolia* L. fibers have potential to application in polymeric matrices as fibrous reinforcement material.

H. M. do Nascimento · S. L. Fávaro (✉)
Departament of Mechanical Engineering, Maringá State University (UEM), Maringá, PR 87020-900, Brazil
e-mail: slfrosa@uem.com

A. dos Santos
Interdisciplinary Department in Field Education, Federal University of Southern Frontier (UFFS), Laranjeiras Do Sul, PR 85301-970, Brazil

V. A. Duarte
Departament of Chemical Engineering, Maringá State University (UEM), Maringá, PR 87020-900, Brazil

P. R. S. Bittencourt
Department of Chemistry, Federal Technological University of Paraná (UTFPR), Medianeira, PR 85884-000, Brazil

E. Radovanovic
Department of Chemistry, Maringá State University (UEM), Maringá, PR 87020-900, Brazil

Graphic abstract

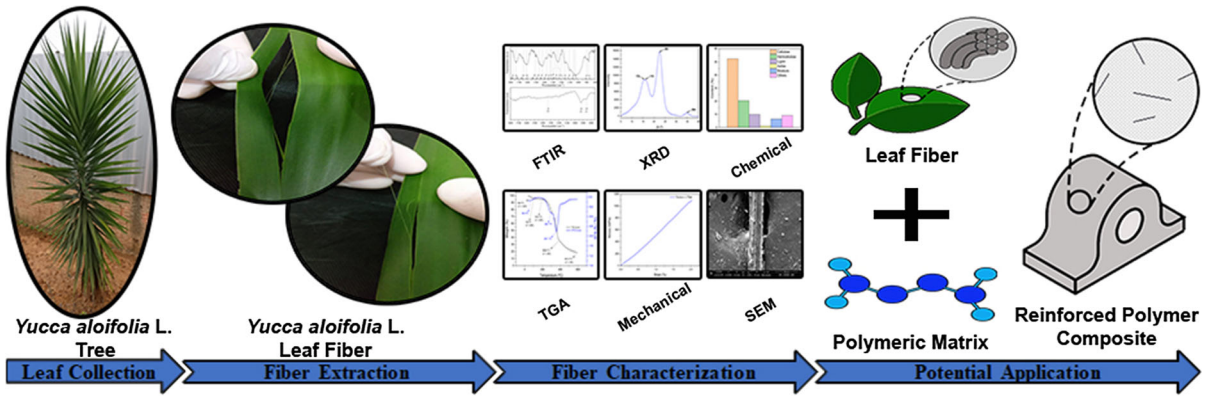

Keywords Natural fibers · Mechanical properties · Chemical properties · Thermal analysis · Crystallinity

Introduction

In recent decades the consumption of polymer matrix composites has increased year by year. The versatility of application of these materials, ease of processing and mechanical behavior, drew attention to its use in various industry segments such as automotive, civil construction, naval and aerospace (Manimaran et al. 2018; Sanjay et al. 2018).

Although synthetic fiber materials have been widely used as reinforcement in polymer matrix composites and have some advantages such as high mechanical strength, high thermal resistance, and good compatibility with polymeric matrices (Sathishkumar et al. 2014; Mahato et al. 2017; Kumar et al. 2020). In the face of the global environmental appeal, alternatives to synthetic fibers commonly used as reinforcement in composites, such as, glass fibers, carbon fibers, aramid fibers had their development accelerated. Then several cellulosic fibers like *Musa textilis* (Abacá), *Hibiscus cannabinus* (Kenaf) and *Boehmeria Nivea* (Rami) started to be used as reinforcement in composite materials and applied in different industrial segments such as automotive, building, furniture, marine and aerospace (Müssig 2010; Salit et al. 2015; Delicano 2018; Kan et al. 2019; Thyavihalli Girijappa et al. 2019; Sanjay et al. 2019; Vinod et al. 2020; Mohd Radzuan et al. 2020).

The use of natural fibers to obtain composites has several economic and sustainable development advantages, mainly due to their characteristics which include excellent mechanical properties, low coast, low density, low abrasiveness, ease of processability, abundance, and biodegradability (Al-Oqla 2017; AL-Oqla and El-Shekeil 2019; AL-Oqla 2020).

Additionally, the use of natural fibers combined with biodegradable resins can increase the sustainability of the use of composite materials giving rise to completely green composites (LeSar and LeSar 2013; Koronis and Silva 2018; AL-Oqla and El-Shekeil 2019; Manimaran et al. 2019; AL-Oqla 2020).The fibers obtained from *Agave sisalana* (Sisal), *Sansevieria cylindrica* (Saint George's Spear) and *Agave tequilana* (Blue Agave), plants of the order Asparagales, have presented promising results as reinforcement in composites. This fact has motivated the search for new species that demonstrate potential for application in polymeric matrix composites (Belouadah et al. 2015; Sreenivasan et al. 2015; Langhorst et al. 2018; Manimaran et al. 2018; Senthilkumar et al. 2018).

The findings about natural fibers revealed their potential as reinforcement material and highlighted their advantages to replace synthetic fibers. The main benefits include the biodegradability, are renewable, present low abrasivity, low cost and low density and have good mechanical properties (Shubhra et al. 2013; Chung et al. 2018; Fangueiro and Rana 2018). As a

result, the demand for materials reinforced with natural fibers grew and the search for news fibers for new applications followed in the same way. (Baskaran et al. 2018).

Thus, to increase the range of reinforcement materials with potential applications in polymer matrix composites, a new source of natural fibers obtained from the leaves of *Yucca aloifolia* L. is presented.

The *Yucca aloifolia* L. belongs to the order of the Asparagales that possesses 1122 plant genera being at least two of them used in the manufacture of composites, the genus Agave and the Sansevieria. The genus *Yucca* belongs to the same order and subfamily as the agaves named Agavoideae (formerly classified as Agavaceae) (Chase et al. 2009, 2016; Albers and Meve 2001; Britannica 2015; Kress 2018; Langhorst et al. 2018; Senthilkumar et al. 2018). The *Yucca aloifolia* L. is one of about 40 species of *Yucca* cataloged. It is a plant originating from Central and North America, recognized mainly for its resistance to water scarcity and soils devoid of nutrients. Although several *Yucca* species are of considerable importance to man and have various uses in ancient indigenous civilizations in the United States and Mexico, only a few studies have been recently developed describing potential applications for *Yucca aloifolia* L., almost exclusively treating the use of the oil extracted from its seeds as a drug (Mokbli et al. 2018) or raw material for the manufacture of biodiesel (Nehdi et al. 2015). Despite this, and for the best of our knowledge, there are not scientific literature describing its application in composites of polymeric matrix. In comparison, some agaves species, such as Sisal and Blue Agave, have been extensively studied and have many publications describing their application in polymeric matrix composites and manufacture of components (Chase et al. 2009, 2016; Albers and Meve 2001; Britannica 2015; Kress 2018; Langhorst et al. 2018; Senthilkumar et al. 2018). Thus, since almost all species of the genus *Yucca* have considerable potential for crop formation and several species are often cultivated as ornamental plants, having spread and naturalized around the world (Albers and Meve 2001), we decided to investigate one of its species as a source of natural fibers for application in polymeric matrix composites.

Materials and methods

Fibers obtainment

The leaves of *Yucca aloifolia* L. were collected in the city of Maringá, Paraná State, Brazil. The leaves of *Yucca aloifolia* L. have two stages described in the literature, at first the leaves are healthy and are in an erect position, forming an angle about 45° in relation to the trunk, in a second stage the leaves start to be curves in direction of the trunk staying in this condition until finally die and dry, remaining attached in the trunk. In this study, the leaves were collected of an adult *Yucca aloifolia* L. plant which has about twenty years and only adults and health leaves between 35 and 45 cm were utilized. The exact age of the leaves cannot be determined, first because the life cycle of one leaf vary compared to another, and second the plant has not been cultivated (Webber 1895).

After being collected, leaves were washed with soap and water and subjected to extraction of the fibers by mechanical pull-out; The extracted fiber was washed with deionized water, and dried at 60 °C for 24 h. This process is summarized in the Fig. 1.

Characterization methods

ATR-FTIR

The fibers of *Yucca aloifolia* L. were characterized using Attenuated Total Reflectance Fourier Transform Infrared Spectroscopy (ATR-FTIR) technique. The measurement was obtained using a Bruker Optics (RAM II FT-Raman Module Vertex Series) instrument, operating in the region 4000–650 cm^{-1}, with a resolution of 4 cm^{-1}.

XRD

The fibers were characterized by X-ray diffraction using a Bragg–Brentano X-ray diffractometer (Shimadzu XRD-6000), with radiation source Cu Kα (λ = 1.5418 Å). The diffractogram was recorded between 5° and 40° (2θ), the acquisition speed was 0.15°/min, the tension and current utilized was 40 kV and 30 mA, respectively.

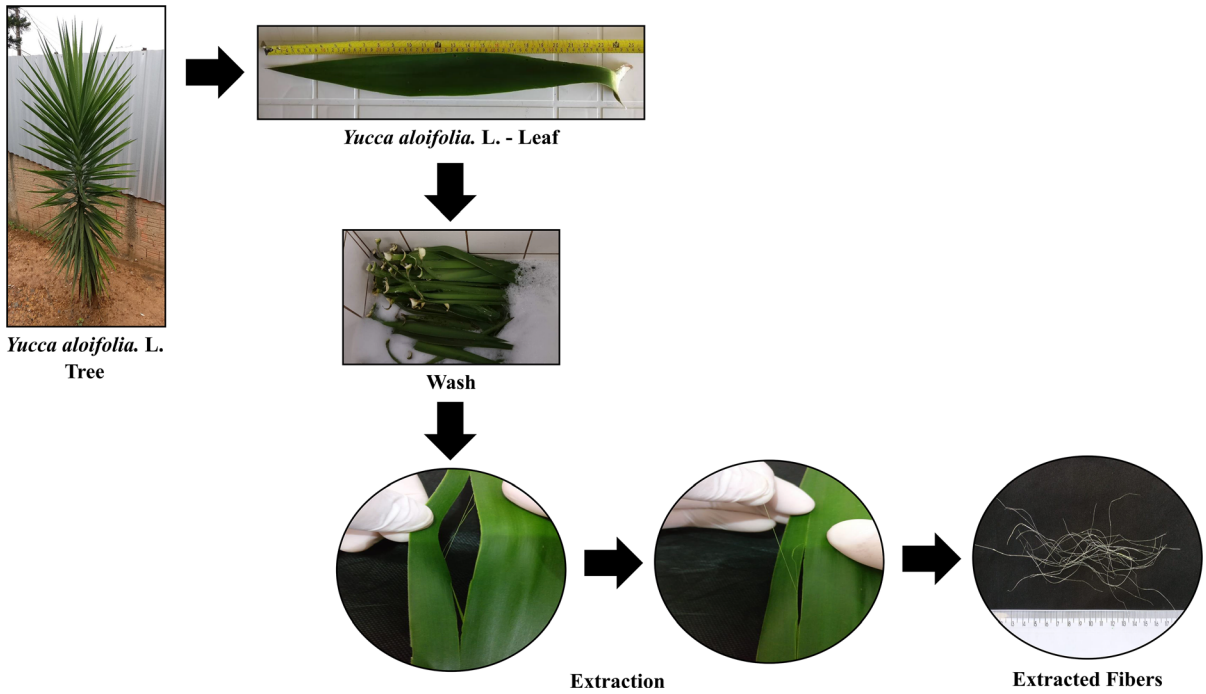

Fig. 1 Fiber extraction of the *Yucca aloifolia* L. leaf

To calculate the crystalline index (CrI) of fibers, the Segal method was used (Segal et al. 1959), the CrI is calculated from the height ratio between the intensity of the crystalline peak corresponding to the Miller indices 200 situated between 2θ = 22–24°, and the intensity of diffraction of the non-crystalline material, which is situated at valley between the peaks corresponding to the Miller indices 110 and 200, near 2θ = 18° (Ling et al. 2019).

The diffraction pattern had the data from a blank run, including the sample holder, subtracted from the data of experimental samples (Hermans and Weidinger 1948; Ling et al. 2019; French 2020). In addition, the experimental data was fitted in MAUD software (Lutterotti et al. 2007) utilizing a cellulose Iβ pattern (French 2014), the experimental and fitted curves were exported and plotted in Origin Software where were performed the follow calculus to CrI and crystallite size.

The crystalline index was calculated using the Eq. (1) (Karimi and Taherzadeh 2016):

$$\boldsymbol{CrI} = \frac{(\boldsymbol{I}_{200} - \boldsymbol{I}_{am})}{\boldsymbol{I}_{200}} \times \mathbf{100} \tag{1}$$

where I_{200} is the maximum peak intensity at 2θ = 22.5° related to the crystalline content and I_{am} represents the intensity of diffraction of the non-crystalline content in 2θ = 19.14°

The crystallite size was calculated using Scherrer's Eq. (2) (Scherrer 1912; French and Santiago Cintrón 2013) rather than MAUD crystallite size values, which are larger than those calculated with the Scherrer equation (Ling et al. 2019), the measure was performed utilizing a Gaussian function in Origin software.

$$\boldsymbol{\tau} = \frac{\boldsymbol{K}.\boldsymbol{\lambda}}{\boldsymbol{\beta} \cdot \cos \boldsymbol{\theta}} \tag{2}$$

where τ is the size perpendicular to the lattice plane, K is the Scherrer's constant taken as 0.9, λ is the wavelength of the radiation source used (1.5418 Å), β is the peak's full-width at half-maximum at (200) reflection for cellulose I in radians, θ is the Bragg angle of the diffraction peak.

Chemical composition

The determination of composition of the fibers in terms of amount of cellulose, hemicellulose and lignin

was performed according to the Van Soest method (Van Soest 1963; Vaz 2016). The method is carried out applying a neutral detergent solution to dissolve easily soluble materials, such as proteins and lipids. Then, the material is subjected to an acidic detergent solution, resulting in the solubilization of hemicellulose. The residue from the acid detergent solution is then treated with sulfuric acid (H_2SO_4) to remove cellulose. The final residual substance is taken to a muffle at 550 °C for 4 h, resulting in the fraction corresponding to insoluble minerals. The material in analysis is weighed before and after each stage, the fractions belonging to each constituent were given by mass difference (Van Soest 1963; Vaz 2016).

TGA

The thermal analysis was held in a simultaneous thermal analyzer from Perkin Elmer (STA 6000) with an open platinum crucible and heating rate of 10 °C/min, in the temperature range from 40 to 600 °C, under an atmosphere of nitrogen flow at 20 ml/min.

Tensile test

The fibers were subjected to tensile testing in a Stable Micro Systems (TA.XT. Plus) texturometer with 50 kgf load cell. The data acquisition occurred at a speed of 6 mm/min following a standard method (ASTM International 2013). Twelve samples were randomly chosen and tested, the free length of samples was 25 mm. The values for force (N) and distance (mm) obtained were subsequently used to perform the calculations of tensile strength (T.S.), Young's modulus (Y.M.) and elongation (EL). The cross-section area of the fibers was obtained by microscopy. For the calculation, Excel and Visual Basic® software were used.

SEM

The morphological study was carried out with FEI (Quanta250) SEM equipment. After the tensile test, the samples were identified and covered with gold by sputtering. The images were obtained towards the length of the fiber and used to determine its cross-section, allowing the determination of T.S., Y.M. and EL. For measurement of fiber cross section values was used the software ImageJ (Schneider et al. 2012). Three measurements were performed on the perpendicular direction of fiber alignment for each one of the fibers. The mean value of the measurements was used as the fiber diameter.

Results and discussion

ATR-FTIR

The spectra were divided in two regions, the fingerprint region that comprises the range of 1800 to 800 cm^{-1} and the region comprised between 3800 and 2750 cm^{-1}. The bands were identified by numbers in Fig. 2. In the region between 2750 to 1800 cm^{-1} no significant bands were found.

The region between 800 and 1800 cm^{-1} contains the largest number of bands identified, most of which are attributed to plant material as bands associated with cellulose, lignin, and hemicellulose. In the spectra can be observed bands attributed to lignin groups such as bands in 1770_{20} cm^{-1} attributable to the stretching of C=O bonds in conjugated ketones, 1738_{19} cm^{-1} attributable to the stretching of C=O bonds in non-conjugated ketones, 1611_{17} cm^{-1} attributable to the stretching of C = C bonds in the aromatic ring syringyl (S), 1507_{16} cm^{-1} assigned to the stretch C=C bonds associated with lignin and 1275_{9} cm^{-1} attributed to C–O bond in aromatic methoxyl groups present in the guaiacyl. Bands attributed to lignin and cellulose present in how 1462_{15} cm^{-1} assigned to asymmetric C–H deformation OCH3, CH2 in the pyran ring, 1423_{14} cm^{-1} ascribed to asymmetric C–H deformation –OCH3, 1372_{13} cm^{-1} flexural CH assigned to cellulose I, II and hemicellulose 1333_{12} cm^{-1} attributed to C–O bond and flexural bending in CH plan cellulose I and II, 1235_{8} cm^{-1} assigned to the syringyl ring and stretching C–O in the lignin and xylan, 1156_{6} cm^{-1} attributable to the asymmetrical stretching C–O–C bond in the cellulose I and II, 1102_{5} cm^{-1} ascribed to aromatic deformation the typical C–H plan units of S and stretching C=O and 1030_{3} cm^{-1} attributed to deformation of the C–O bond in the cellulose I and II and finally bands allocated cellulose as found at 1317_{11} cm^{-1} CH_2 bending attributed to the cellulose I and II, 1280_{10} cm^{-1} assigned to the deformation CH cellulose I and II, 1201_{7} cm^{-1} assigned to the bending plane –OH unoxidized cellulose, 1052_{4} cm^{-1} bending

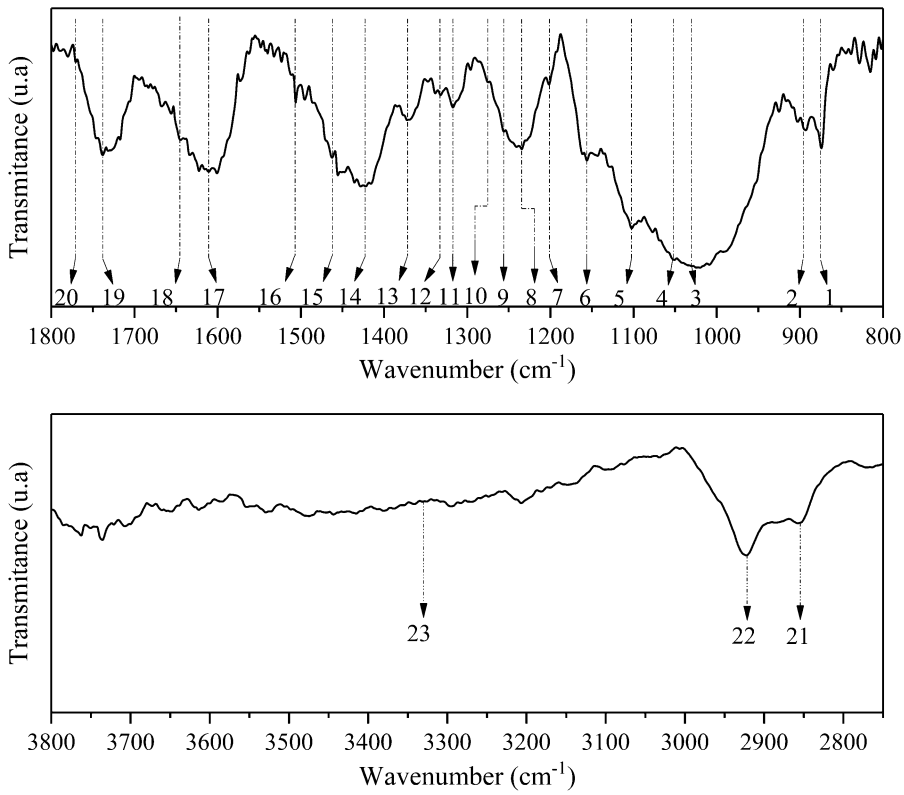

Fig. 2 ATR-FTIR spectrum of *Yucca aloifolia* L. fibers

attributed to C–O valence linkage, mainly C(3)–O(3)H and 895_2 cm^{-1} assigned to amorphous cellulose. Besides that, bands in 1645_{18} cm^{-1}, assigned to linked water at lignin or cellulose, and in 875_1 cm^{-1}, assigned to bending of the aromatic group in the guaiacyl are noted. (Coseri et al. 2015; Chimeni et al. 2016; Liu et al. 2017; Maulidiyah et al. 2017; Achinivu 2018; Hospodarova et al. 2018; Sanjay et al. 2018; Hemmati et al. 2019).

The region between 3800 and 2750 cm^{-1} is mainly related to the stretching of OH and CH groups. In this region, it possible to observe bands of 2922_{22} cm^{-1} ascribed to the symmetrical stretching CH aromatic methoxyl groups and methyl groups and methylene side chains and 2851_{21} cm^{-1} attributable to the asymmetrical stretching CH aromatic methoxyl groups and methyl groups and methylene side chains. The wideband in 3330_{23} cm^{-1} is assigned to stretching of the OH bond of hydroxyl groups, the increase in the intensity of this band indicator longer exposure OH (Coseri et al. 2015; Chimeni et al. 2016; Liu et al. 2017; Maulidiyah et al. 2017; Achinivu 2018; Hospodarova et al. 2018; Sanjay et al. 2018; Hemmati et al. 2019). With the basis of the analysis results, it is possible to confirm the presence of the main constituents of lignocellulosic fibers, cellulose, hemicellulose and lignin in *Yucca aloifolia* L. fibers. The summary of the band's positions and assignments are presented in Table 1.

X-ray diffraction analysis

In the X-ray diffractogram of *Yucca aloifolia* L. fibers in Fig. 3 is possible to observe the presence of peaks related to the crystalline planes at the following Bragg angles (2θ): 15.5° (1 $\bar{1}$ 0); 16.7° (110); 22.5° (200); and 34.8° (004) (Yue et al. 2012; French and Santiago Cintrón 2013; French 2014; Ling et al. 2019; del Cerro et al. 2020). The peaks related at planes (1 $\bar{1}$ 0) and (110) has overlapped reflection, the overlapped of reflections is influenced by crystallite size which is very small in cellulose samples, about 20–50 Å (Thygesen et al. 2005), the accomplished refinement helped to make them distinguishable. The peaks found are related to crystallographic planes of the cellulose Iβ (French 2014). The preferred orientation is an

Table 1 IR assignments for *Yucca aloifolia* L. fibers

Index number	Wavenumber (cm^{-1})	Band assignment	Band position	Reference
1	875	Deformation outside plane C–H in positions 2, 5 and 6 in guaiacyl units	875	Maulidiyah et al. (2017), Achinivu (2018), Hospodarova et al. (2018)
2	895	Associated with β-glycosidic amorphous cellulose bonds	895	Chimeni et al. (2016), Liu et al. (2017), Hemmati et al. (2019)
3	1047–1004	Deformation of the C–O bond in cellulose I and II	1030	El Oudiani et al. (2017), Liu et al. (2017), Achinivu (2018), Hemmati et al. (2019)
4	1060–1015	Valence bond stretching C–O mainly of C(3)–O(3)H	1052	El Oudiani et al. (2017), Hemmati et al. (2019)
5	1128–1110	C–H aromatic deformation in the typical plane for Syringil and stretching units of CcO	1102	El Oudiani et al. (2017), Hemmati et al. (2019)
6	1162–1125	Asymmetric stretching of the C–O–C bond in cellulose I and II	1156	Chimeni et al. (2016), El Oudiani et al. (2017), Boukir et al. (2019), Hemmati et al. (2019)
7	1201	Bending in the –OH plane of non–oxidized cellulose	1201	Coseri et al. (2015), Hemmati et al. (2019)
8	1235–1230	Syringyl ring and C–O stretching in lignin and xylan	1235	Kurian et al. (2015), El Oudiani et al. (2017)
9	1268	C–O binding in aromatic methoxyl groups of guaiacyl	1275	Kurian et al. (2015); El Oudiani et al. (2017), Boukir et al. (2019)
10	1282–1277	CH deformation in cellulose I and II	1280	El Oudiani et al. (2017), Heinze et al. (2018)
11	1315	Deformation of CH2 in cellulose I and II	1317	Kurian et al. (2015), El Oudiani et al. (2017), Boukir et al. (2019)
12	1335–1320	C–O stretching and bending in the CH plane of cellulose I and II	1333	El Oudiani et al. (2017), Hospodarova et al. (2018)
13	1375–1365	C–H bending in cellulose I, II and hemicellulose	1372	El Oudiani et al. (2017), Hospodarova et al. (2018), Boukir et al. (2019)
14	1430–1422	Asymmetric deformation of C–H at –OCH3	1423	El Oudiani et al. (2017), Hospodarova et al. (2018), Boukir et al. (2019)
15	1470–1455	Asymmetric deformation of C–H in –OCH3, CH2 in pyran ring	1462	El Oudiani et al. (2017), Boukir et al. (2019)
16	1515–1505	Bonding stretching C = C associated with guaicyl	1507	Chimeni et al. (2016), El Oudiani et al. (2017), Boukir et al. (2019)
17	1610–1590	Stretching of C = C bonds in the aromatic syringyl ring	1611	Coseri et al. (2015), El Oudiani et al. (2017)
18	1650–1640	Water associated with lignin or cellulose	1645	El Oudiani et al. (2017), Hyness et al. (2018), Boukir et al. (2019)
19	1740–1720	Stretching of C = O bonds on ketones not conjugated	1738	El Oudiani et al. (2017), Hyness et al. (2018), Boukir et al. 2019)
20	1770–1760	Stretching of C = O bonds in conjugated ketones	1770	(El Oudiani et al. 2017; Heinze et al. 2018)
21	2840–2835	Asymmetrical stretching of CH in aromatic methoxyl groups and side chain methyl and methylene groups	2851	El Oudiani et al. (2017), Achinivu (2018), Hyness et al. (2018)
22	2938–2920	Symmetric stretching of CH in aromatic methoxyl groups and side chain methyl and methylene groups	2922	El Oudiani et al. (2017), Achinivu (2018), Hyness et al. (2018)
23	3700–3000	Deformation of the O–H bond in hydroxyl groups	3330	El Oudiani et al. (2017), Achinivu (2018), Hyness et al. (2018)

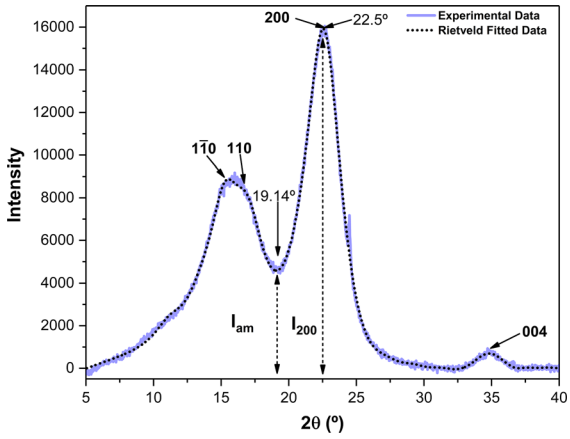

Fig. 3 Diffractogram pattern of *Yucca aloifolia* L. fibers and the Rietveld fitted pattern

inherent factor in cellulosic samples, in this work the relative heights between the overlapping peaks and the peak (200) can be an indicator of its occurrence (Ling et al. 2019; French 2020).

The crystallinity of natural fibers is directly linked to the mechanical behavior, higher cellulose crystallinity results in increased of properties as Young's modulus, tensile strength and hardness (Latif et al. 2019; Rongpipi et al. 2019; Todkar and Patil 2019). In this way these features can be very desirable when it is intended to use natural fibers as a reinforcement in polymeric matrix composites (Sanjay et al. 2018; Lotfi et al. 2019; Gholampour and Ozbakkaloglu 2020). However, it is an extremely important factor, various authors report that the measured crystallinity of cellulose can differ significantly depending on the technique and analysis approach used, limiting the results comparison, even when the same data was used (Karimi and Taherzadeh 2016; Rongpipi et al. 2019).

The CrI of *Yucca aloifolia* L. fibers calculated by Segal method was 69.43% and according to Scherrer equation the crystallite size is approximately 24.6 Å for *Yucca aloifolia* L. fibers. The experimental and fitted data are shown in Fig. 3.

Chemical composition analysis

The chemical composition in weight percent (wt%) of the *Yucca aloifolia* L. fibers (F-Yucca) is shown in Table 2.

The comparison among the values obtained to cellulose, hemicellulose and lignin, for other untreated fibers and *Yucca aloifolia* L., is presented in Table 3. The cellulose, lignin and hemicelluloses content are close to those found in the kenaf fibers, that are widely used in polymer matrix composites (Nematollahi et al. 2019; Radzuan et al. 2019; Mohd Radzuan et al. 2020). Compared with the sisal fibers, that belongs to the same order and subfamily (Agavoideae), the *Yucca aloifolia* L. fibers have cellulose content 14.3% lower, while the hemicellulose and lignin have higher values, 43.9% and 20%, respectively.

Generally, fibers with high cellulose content have higher mechanical properties compared to fibers with less cellulose. A high hemicellulose and lignin content is undesirable for use in polymer matrix composites, because they are more susceptible to thermal degradation and act as igniters increasing the thermal degradation of cellulose (Fan and Fu 2017; Jawaid et al. 2019). However, several factors may be related to the contents of the components found in natural fibers, among them are climatic factors, environmental, or even the age of the plant (Fan and Fu 2017; Jawaid et al. 2019).

Thermogravimetric analysis

TG-DTG curves of the *Yucca aloifolia* L. fibers (F-Yucca) are shown in Fig. 4. It is possible to observe that fibers have four weight loss stages. In the first stage, which occurred below 100 °C, the evaporation of water and volatile compounds present in the fibers occurred, being 4% of the weight lost in this step (Ornaghi et al. 2014). Lower weight loss on this temperature range indicates lower hydrophilicity of the fibers, this being a factor beneficial for use in polymer composites (Fernandes et al. 2013; Chandrasekar et al. 2017). In the second stage, the weight loss presented a maximum rate at 294.7 °C, in this temperature range occurs the depolymerization of glycosidic bonds in hemicellulose and pectin (Fernandes et al. 2013; Indran and Raj 2015; Chandrasekar et al. 2017). The third step of weight loss is related to cellulose degradation that occurred between 310 and 390 °C, with maximum degradation rate at 357.7 °C. Higher temperatures of cellulose degradation are related to the greater thermal stability of the fiber (Fernandes et al. 2013; Indran and Raj 2015; Chandrasekar et al. 2017). The fourth step occurred over to 390 °C, is related to oxidative degradation of lignin and residual of fibers carbonized, corresponding of

Table 2 Chemical composition of *Yucca aloifolia* L. fibers

Sample	Cellulose (wt%)	Hemicellulose (wt%)	Lignin (wt%)	Ashes (wt%)	Moisture (wt%)	Others (wt%)
F-Yucca	52.54	20.53	10.03	1.12	6.56	9.22

Table 3 Typical chemical compositions for natural fibers

Natural fiber	Cellulose (%)	Hemicellulose (%)	Lignin (%)	References
Bagasse	37	21	22	Indran and Raj (2015), Latif et al. (2019)
Bamboo	34.5	20.5	26	Fiore et al. (2014), Indran and Raj (2015), Latif et al. (2019)
Banana	62.4	12.5	7.5	Indran and Raj (2015), Latif et al. (2019)
Cotton	89	4	0.75	Fiore et al. (2014), Indran and Raj (2015), Latif et al. (2019)
Curauá	73.6	5	7.5	Indran and Raj (2015), Latif et al. (2019), Moshi et al. (2020)
Linen	70.5	16.5	2.5	Indran and Raj (2015), Latif et al. (2019), Moshi et al. (2020
Hemp	81	20	4	Suryanto et al. (2014), Indran and Raj (2015), Latif et al. (2019)
Jute	67	16	9	Indran and Raj (2015), Rajeshkumar et al. (2016), Latif et al. (2019)
Kenaf	53.5	21	17	Indran and Raj (2015), Latif et al. (2019)
Piassava	28.6	25.8	45	Indran and Raj (2015), Rajeshkumar et al. (2016), Latif et al. (2019), Moshi et al. (2020)
Pineapple	80.5	17.5	8.3	Indran and Raj (2015), Latif et al. (2019)
Ramie	72	14	0.8	Fiore et al. (2014), Indran and Raj (2015), Latif et al. (2019), Moshi et al. (2020)
Sisal	60	11.5	8	Fiore et al. (2014), Suryanto et al. (2014), Indran and Raj (2015), Latif et al. (2019)
Yucca aloifolia L	52.5	20.5	10	Present work

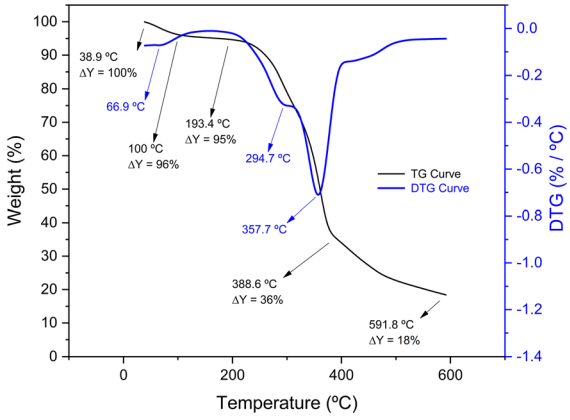

Fig. 4 TG-DTG curve of *Yucca aloifolia* L. fibers

18% of the total weight at the end of the process at 591.8 °C. (Indran and Raj 2015; Jordá-Vilaplana et al. 2017; Wang et al. 2018).

Thermal characterization of the natural fibers is particularly important when it is aiming to apply them in composite materials since in various manufacturing processes are used high temperatures. Thus, the evaluation of the thermal behavior at different temperatures is fundamental and can help to determine the optimum thermal condition to fiber application in different polymeric matrices preventing it from occurring thermal degradation (Belouadah et al. 2015).

The temperature at which the degradation of hemicellulose and pectin begins in the fibers of *Yucca aloifolia* L., around 193 °C, is higher than the melting temperature of several polymeric materials, allowing the fibers to be applied in a wide range of polymeric materials without suffering thermal degradation. Thermoplastics, such as polypropylene (PP), polyethylene (PE) and polyvinyl chloride (PVC), as well as

thermosets, such as epoxy, phenolic and polyester resins (Callister and Rethwisch 2015), are widely used in obtaining composites reinforced with natural fibers (Chauhan et al. 2019) and can be reinforced with *Yucca aloifolia* L. fibers.

Tensile properties

Based on the fiber diameters obtained by SEM images, the fiber mechanical properties are shown in Table 4. The high variability found in the results is expected in mechanical tests of natural fibers. It is related to the characteristics of this type of fiber, such as structural imperfections, cross-sectional variability along the length of fiber, shown in Fig. 7, and variability of the geometric profile (Alves Fidelis et al. 2013; Noda et al. 2016). The stress/strain patterns are shown in Fig. 5.

The comparison between the values for tensile strength, Young's modulus and deformation of other natural fibers and *Yucca aloifolia* L. fibers are shown in Table 5. The values obtained portray that the tensile strength obtained is the fourth largest among the compared fibers, being smaller than typical values founded for pineapple, ramie and Curauá fibers. Therefore, it can be concluded that *Yucca aloifolia* L. fibers have mechanical characteristics similar to the other fibers applied in polymer matrix composites.

SEM

The morphological analysis revealed the presence of parenchymal cell residues and that the fiber structure is completely joined by lignin, forming uneven and continuous filaments along the length of the fiber (Neto et al. 2012; Ramphul et al. 2017). Fiber morphology is a determining factor in its application as reinforcement in composite materials (Indran and Raj 2015). Although the low roughness observed on the surface of the fibers and the significant presence of non-cellulosic constituents indicates that the fibers need to undergo surface modification, such as a fiber cleaning process, before to be applied in polymeric matrix composites. A fiber surface treatment is essential for achieving good interfacial adhesion between the fiber and the matrix (Moshi et al. 2020).

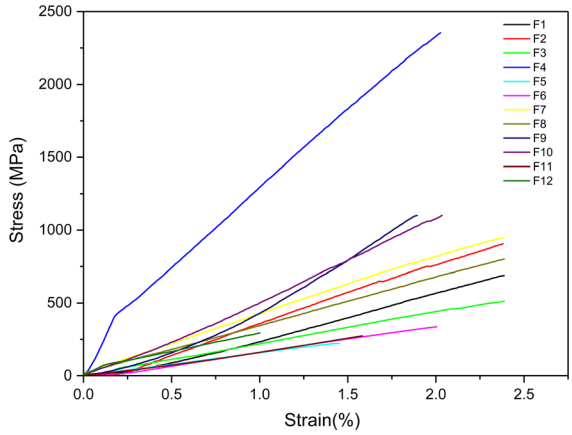

Fig. 5 Single fibers stress/strain curves of *Yucca aloifolia* L.

Prior knowledge of the fiber's morphological characteristics is extremely important to decide the best treatments and applications in composite materials. Analyzing the treatments applied to the fibers that belong to the same family of *Yucca aloifolia* L. as *Agave Sisalana* (Senthilkumar et al. 2018; Melkamu et al. 2019) and *Agave Americana* L. (Ben Sghaier et al. 2012; El Oudiani et al. 2012; Madhu et al. 2020), very desirable results can be observed in the fibers that have gone through the mercerization process, which in some cases was able to provide cleaning of the fibers while maintaining their mechanical characteristics in addition to provide improvement in its thermal resistance characteristics. The scanning electron micrographs of the *Yucca aloifolia* L. fibers are shown in Fig. 6.

The cross-sectional analyses of *Yucca aloifolia* L. fibers revealed a large variation in the dimensions of the sections when compared to each other, which is expected in natural fibers and may influence their mechanical behavior. The variations in the section of

Table 4 Tensile properties of Single fibers of *Yucca aloifolia* L

Yucca aloifolia L	Tensile strength (MPa)	Young's modulus (GPa)	Elongation (%)	Diameter (μm)
Mean	801 ± 587	39 ± 28	2 ± 0.5	81 ± 33

Table 5 Typical average mechanical properties of natural fibers

Natural fiber	Tensile strength (MPa)	Young's modulus (GPa)	Elongation (%)	References
Bagasse	290	17	–	Suryanto et al. (2014), Latif et al. (2019)
Bamboo	503–575	27	1.4	Fiore et al. (2014), Balaji and Nagarajan (2017), Shanmugasundaram et al. (2018)
Banana	721	29	2	Reddy et al. (2014), Latif et al. (2019)
Cotton	500	8	7	Fiore et al. (2014), Suryanto et al. (2014), Hyness et al. (2018)
Curauá	543–825	9	7.5	Alves Fidelis et al. (2013), Latif et al. (2019)
Hemp	530	45	3	Balaji and Nagarajan (2017), Hyness et al. (2018)
Jute	325	37.5	2.5	Fiore et al. (2014), Hyness et al. 2018)
Kenaf	743	41	1.6	Reddy et al. (2014), Hyness et al. (2018)
Piassava	77–138	2.83	5	Fiore et al. (2014), Latif et al. (2019)
Pineapple	1020	71	0.8	Reddy et al. (2014), Hyness et al. (2018)
Ramie	925	23	3.7	Fiore et al. (2014), Balaji and Nagarajan (2017), Hyness et al. (2018)
Sisal	460–700	15.5	3–7	Fiore et al. (2014), Reddy et al. (2014), Hyness et al. (2018), Latif et al. (2019)
Yucca aloifolia L	801	39	2	Present work

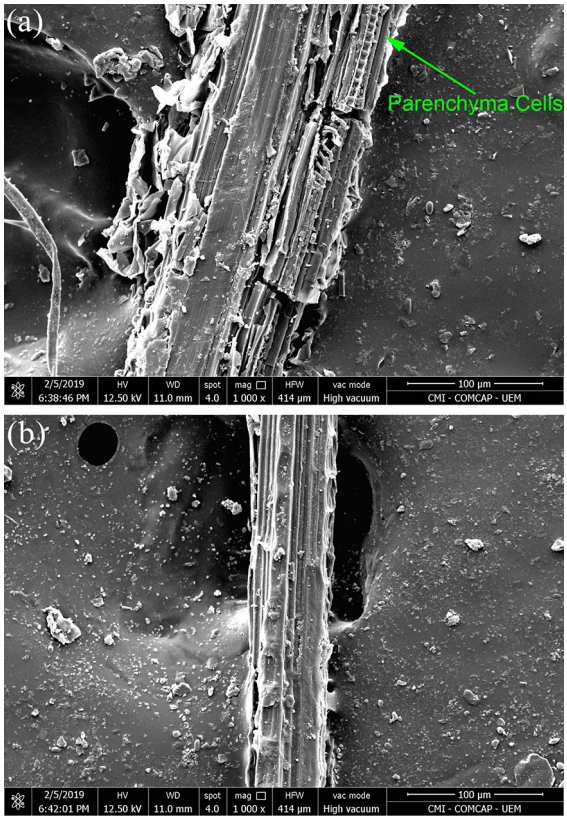

Fig. 6 SEM images of *Yucca aloifolia* L. fibers

the fibers are mainly related to the way the fibers were extracted, to the species of the plant and to factors related to its growth such as the environment where the plant grown and its age (Baskaran et al. 2018; Lotfi et al. 2019; Manimaran et al. 2019; Vinod et al. 2020). Section micrographs of the *Yucca aloifolia* L. fibers are shown in Fig. 7. The fracture region of fiber after tensile test were presented in Fig. 8.

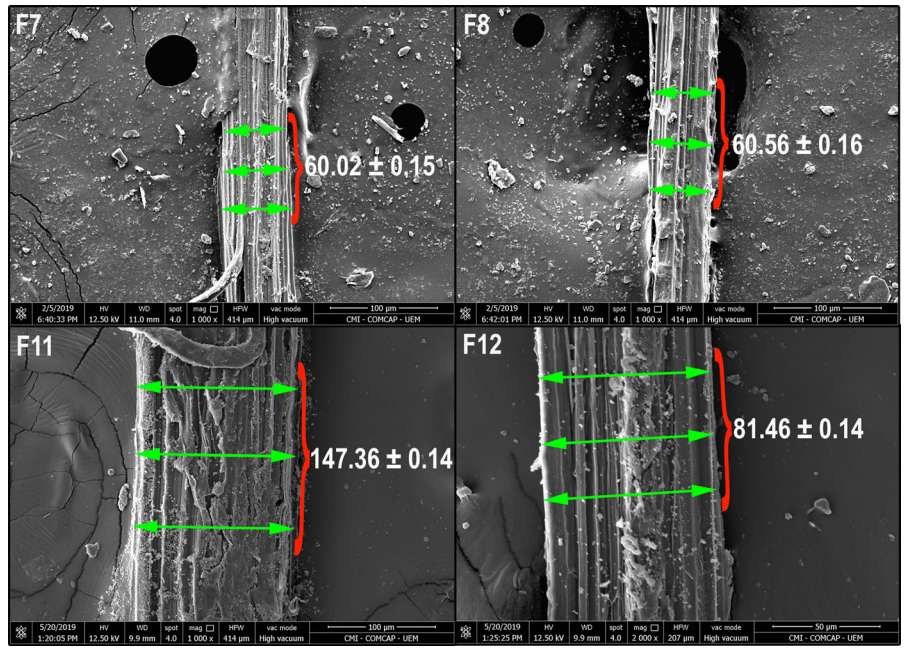

Fig. 7 SEM images of sectional variation of *Yucca aloifolia* L. fibers

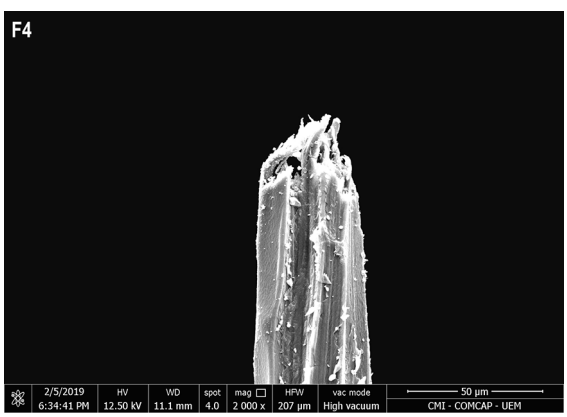

Fig. 8 SEM image of fracture region of *Yucca aloifolia* L. fiber

Conclusion

Physicochemical, thermal, mechanical and morphological analyses revealed that the fibers extracted from the leaves of *Yucca aloifolia* L., compared with other natural fibers already used, have the potential for application in polymeric matrix composites.

The results obtained in the ATR-FTIR characterization showed the presence of the main constituents of lignocellulosic fibers, cellulose, hemicellulose, and lignin in the fibers of *Yucca aloifolia* L. The chemical characterization indicates that the fibers are constituted by a high amount of cellulose, about 52.5%, being the crystallinity index of the cellulose obtained through XRD analysis of 69.43%. The thermal analysis performed through TGA, reveals excellent thermal stability of the fibers up to temperatures of 193.4 °C, allowing the fibers to be applied in various polymeric materials.

The mechanical characterization of the fibers pointed to a very desirable mechanical behavior in reinforcements applied in composites obtaining high average values in comparison with other natural fibers such as 801 MPa for tensile strength and 39 GPa for Young's module, the elongation of 2%, the mechanical properties found for *Yucca aloifolia* L. fibers exceed those found in fibers commonly used in polymeric composites such as sisal, jute and hemp.

The images captured in SEM analyses revealed the presence of a large amount of non-cellulosic constituents present on the surface of the fibers.

Based on the obtained results, it can be stated that the fibers of *Yucca aloifolia* L. have potential application in composites of polymeric matrix.

Acknowledgements The authors are grateful to Capes and CNPq/Brazil for funding this work and COMCAP – UEM, by SEM microscopies.

Declarations

Conflict of interest The authors declare that they have no conflict of interest.

References

Achinivu EC (2018) Protic ionic liquids for lignin extraction—a lignin characterization study. Int J Mol Sci. https://doi.org/10.3390/ijms19020428

Albers F, Meve U (2001) Illustrated handbook of succulent plants: monocotyledons, 1st edn. Springer, Berlin, Heidelberg

Al-Oqla FM (2017) Investigating the mechanical performance deterioration of Mediterranean cellulosic cypress and pine/polyethylene composites. Cellulose 24:2523–2530. https://doi.org/10.1007/s10570-017-1280-3

Al-Oqla FM (2020) Flexural characteristics and impact rupture stress investigations of sustainable green olive leaves biocomposite materials. J Polym Environ. https://doi.org/10.1007/s10924-020-01889-3

Al-Oqla FM, El-Shekeil YA (2019) Investigating and predicting the performance deteriorations and trends of polyurethane bio-composites for more realistic sustainable design possibilities. J Clean Prod 222:865–870. https://doi.org/10.1016/j.jclepro.2019.03.042

Alves Fidelis ME, Pereira TVC, Gomes ODFM et al (2013) The effect of fiber morphology on the tensile strength of natural fibers. J Mater Res Technol 2:149–157. https://doi.org/10.1016/j.jmrt.2013.02.003

ASTM International (2013) ASTM C1557, 2003, standard test method for tensile strength and Young's modulus of fibres. ASTM. https://doi.org/10.1520/C1557-14.2

Balaji AN, Nagarajan KJ (2017) Characterization of alkali treated and untreated new cellulosic fiber from Saharan aloe vera cactus leaves. Carbohydr Polym 174:200–208. https://doi.org/10.1016/j.carbpol.2017.06.065

Baskaran PG, Kathiresan M, Senthamaraikannan P, Saravanakumar SS (2018) Characterization of new natural cellulosic fiber from the bark of *Dichrostachys Cinerea*. J Nat Fibers 15:62–68. https://doi.org/10.1080/15440478.2017.1304314

Belouadah Z, Ati A, Rokbi M (2015) Characterization of new natural cellulosic fiber from *Lygeum spartum* L. Carbohydr Polym 134:429–437. https://doi.org/10.1016/j.carbpol.2015.08.024

Ben Sghaier AEO, Chaabouni Y, Msahli S, Sakli F (2012) Morphological and crystalline characterization of NaOH and NaOCl treated *Agave americana* L. fiber. Ind Crops Prod 36:257–266. https://doi.org/10.1016/j.indcrop.2011.09.012

Boukir A, Fellak S, Doumenq P (2019) Structural characterization of *Argania spinosa* Moroccan wooden artifacts during natural degradation progress using infrared spectroscopy (ATR-FTIR) and X-Ray diffraction (XRD). Heliyon 5:e02477. https://doi.org/10.1016/j.heliyon.2019.e02477

Callister WD, Rethwisch DG (2015) Fundamentals of materials science and engineering an integrated approach, 5[a]. Hoboken, NJ, USA

Chandrasekar M, Ishak MR, Sapuan SM et al (2017) A review on the characterisation of natural fibres and their composites after alkali treatment and water absorption. Plast Rubber Compos 46:119–136. https://doi.org/10.1080/14658011.2017.1298550

Chase MW, Christenhusz MJM, Fay MF et al (2009) An update of the angiosperm phylogeny group classification for the orders and families of flowering plants: APG III. Bot J Linn Soc 161:105–121. https://doi.org/10.1111/j.1095-8339.2009.00996.x

Chase MW, Christenhusz MJM, Fay MF et al (2016) An update of the angiosperm phylogeny group classification for the orders and families of flowering plants: APG IV. Bot J Linn Soc 181:1–20. https://doi.org/10.1111/boj.12385

Chauhan V, Kärki T, Varis J (2019) Review of natural fiber-reinforced engineering plastic composites, their applications in the transportation sector and processing techniques. J Thermoplast Compos Mater. https://doi.org/10.1177/0892705719889095

Chimeni DY, Toupe JL, Dubois C, Rodrigue D (2016) Effect of hemp surface modification on the morphological and tensile properties of linear medium density polyethylene (LMDPE) composites. Compos Interfaces 23:405–421. https://doi.org/10.1080/09276440.2016.1144163

Chung TJ, Park JW, Lee HJ et al (2018) The improvement of mechanical properties, thermal stability, and water absorption resistance of an eco-friendly PLA/kenaf biocomposite using acetylation. Appl Sci. https://doi.org/10.3390/app8030376

Coseri S, Biliuta G, Zemljič LF et al (2015) One-shot carboxylation of microcrystalline cellulose in the presence of nitroxyl radicals and sodium periodate. RSC Adv 5:85889–85897. https://doi.org/10.1039/c5ra16183e

De Carvalho Neto AGV, Ganzerli TA, Cardozo AL et al (2014) Development of composites based on recycled polyethylene/sugarcane bagasse fibers. Polym Compos 35:768–774. https://doi.org/10.1002/pc.22720

del Cerro DR, Koso TV, Kakko T et al (2020) Crystallinity reduction and enhancement in the chemical reactivity of cellulose by non-dissolving pre-treatment with tetrabutylphosphonium acetate. Cellulose 27:5545–5562. https://doi.org/10.1007/s10570-020-03044-6

Delicano JA (2018) A review on abaca fiber reinforced composites. Compos Interfaces 25:1039–1066. https://doi.org/10.1080/09276440.2018.1464856

El Oudiani A, Chaabouni Y, Msahli S, Sakli F (2012) Mercerization of *Agave americana* L. fibers. J Text Inst 103:565–574. https://doi.org/10.1080/00405000.2011.590010

El Oudiani A, Msahli S, Sakli F (2017) In-depth study of agave fiber structure using Fourier transform infrared spectroscopy. Carbohydr Polym 164:242–248. https://doi.org/10.1016/j.carbpol.2017.01.091

Fan M, Fu F (eds) (2017) advanced high strength natural fibre composites in construction. Elsevier, Duxford, UK

Fangueiro R, Rana S (2018) Advances in natural fibre composites. Springer International Publishing, Berlin

Fernandes EM, Mano JF, Reis RL (2013) Hybrid cork-polymer composites containing sisal fibre: Morphology, effect of the fibre treatment on the mechanical properties and tensile failure prediction. Compos Struct 105:153–162. https://doi.org/10.1016/j.compstruct.2013.05.012

Fiore V, Scalici T, Valenza A (2014) Characterization of a new natural fiber from *Arundo donax* L. as potential reinforcement of polymer composites. Carbohydr Polym 106:77–83. https://doi.org/10.1016/j.carbpol.2014.02.016

French AD (2014) Idealized powder diffraction patterns for cellulose polymorphs. Cellulose 21:885–896. https://doi.org/10.1007/s10570-013-0030-4

French AD (2020) Increment in evolution of cellulose crystallinity analysis. Cellulose 27:5445–5448. https://doi.org/10.1007/s10570-020-03172-z

French AD, Santiago Cintrón M (2013) Cellulose polymorphy, crystallite size, and the segal crystallinity index. Cellulose 20:583–588. https://doi.org/10.1007/s10570-012-9833-y

Gholampour A, Ozbakkaloglu T (2020) A review of natural fiber composites: properties, modification and processing techniques, characterization, applications. Springer, US

Heinze T, El Seoud OA, Koschella A (2018) Cellulose Derivatives. Springer, Cham

Hemmati F, Jafari SM, Taheri RA (2019) Optimization of homogenization-sonication technique for the production of cellulose nanocrystals from cotton linter. Int J Biol Macromol 137:374–381. https://doi.org/10.1016/j.ijbiomac.2019.06.241

Hermans PH, Weidinger A (1948) Quantitative x-ray investigations on the crystallinity of cellulose fibers. A background analysis. J Appl Phys 19:491–506. https://doi.org/10.1063/1.1698162

Hospodarova V, Singovszka E, Stevulova N (2018) Characterization of cellulosic fibers by FTIR spectroscopy for their further implementation to building materials. Am J Anal Chem 09:303–310. https://doi.org/10.4236/ajac.2018.96023

Hyness NRJ, Vignesh NJ, Senthamaraikannan P et al (2018) Characterization of new natural cellulosic fiber from *Heteropogon Contortus* plant. J Nat Fibers 15:146–153. https://doi.org/10.1080/15440478.2017.1321516

Indran S, Raj RE (2015) Characterization of new natural cellulosic fiber from *Cissus quadrangularis* stem. Carbohydr Polym 117:392–399. https://doi.org/10.1016/j.carbpol.2014.09.072

Jawaid M, Thariq M, Saba N (eds) (2019) Failure analysis in biocomposites, fibre-reinforced composites and hybrid composites, 1st edn. Woodhead Publishing, Duxford, UK

Jordá-Vilaplana A, Carbonell-Verdú A, Samper MD et al (2017) Development and characterization of a new natural fiber reinforced thermoplastic (NFRP) with *Cortaderia selloana* (Pampa grass) short fibers. Compos Sci Technol 145:1–9. https://doi.org/10.1016/j.compscitech.2017.03.036

Kan Z, Shi H, Zhao E, Wang H (2019) Preparation and performance of different modified ramie fabrics reinforced anionic polyamide-6 composites. Processes 7:1–15. https://doi.org/10.3390/pr7040226

Karimi K, Taherzadeh MJ (2016) A critical review of analytical methods in pretreatment of lignocelluloses: composition, imaging, and crystallinity. Bioresour Technol 200:1008–1018. https://doi.org/10.1016/j.biortech.2015.11.022

Koronis G, Silva A (2019) Green composites for automotive applications. Elsevier

Kress WJ (2018) "Asparagales". Encyclopedia Britannica. https://www.britannica.com/plant/Asparagales. Accessed 28 Nov 2019

Kumar A, Sharma K, Dixit AR (2020) Carbon nanotube- and graphene-reinforced multiphase polymeric composites: review on their properties and applications. J Mater Sci 55:2682–2724. https://doi.org/10.1007/s10853-019-04196-y

Kurian JK, Gariepy Y, Orsat V, Raghavan GSV (2015) Microwave-assisted lime treatment and recovery of lignin from hydrothermally treated sweet sorghum bagasse. Biofuels 6:341–355. https://doi.org/10.1080/17597269.2015.1110775

Langhorst AE, Burkholder J, Long J et al (2018) Blue-agave fiber-reinforced polypropylene composites for automotive applications. BioResources 13:820–835. https://doi.org/10.15376/biores.13.1.820-835

Latif R, Wakeel S, Khan NZ et al (2019) Surface treatments of plant fibers and their effects on mechanical properties of fiber-reinforced composites: a review. J Reinf Plast Compos 38:15–30. https://doi.org/10.1177/0731684418802022

LeSar R, LeSar R (2013) Materials selection and design. Introd to Comput Mater Sci. https://doi.org/10.1017/cbo9781139033398.015

Ling Z, Wang T, Makarem M et al (2019) Effects of ball milling on the structure of cotton cellulose. Cellulose 26:305–328. https://doi.org/10.1007/s10570-018-02230-x

Liu W, Fei M, Ban Y et al (2017) Preparation and evaluation of green composites from microcrystalline cellulose and a soybean-oil derivative. Polymers (Basel). https://doi.org/10.3390/polym9100541

Lotfi A, Li H, Dao DV, Prusty G (2019) Natural fiber-reinforced composites: a review on material, manufacturing, and machinability. J Thermoplast Compos Mater. https://doi.org/10.1177/0892705719844546

Lutterotti L, Bortolotti M, Ischia G et al (2007) Rietveld texture analysis from diffraction images. Zeitschrift fur Krist Suppl 1:125–130. https://doi.org/10.1524/zksu.2007.2007.suppl_26.125

Madhu P, Sanjay MR, Jawaid M et al (2020) A new study on effect of various chemical treatments on *Agave americana* fiber for composite reinforcement: physico-chemical, thermal, mechanical and morphological properties. Polym Test 85:106437. https://doi.org/10.1016/j.polymertesting.2020.106437

Mahato KK, Dutta K, Ray BC (2017) High-temperature tensile behavior at different crosshead speeds during loading of glass fiber-reinforced polymer composites. J Appl Polym Sci. https://doi.org/10.1002/app.44715

Manimaran P, Prithiviraj M, Saravanakumar SS et al (2018) Physicochemical, tensile, and thermal characterization of new natural cellulosic fibers from the stems of *Sida cordifolia*. J Nat Fibers 15:860–869. https://doi.org/10.1080/15440478.2017.1376301

Manimaran P, Saravanan SP, Sanjay MR et al (2019) Characterization of new cellulosic fiber: *Dracaena reflexa* as a reinforcement for polymer composite structures. J Mater

Res Technol 8:1952–1963. https://doi.org/10.1016/j.jmrt.2018.12.015

Maulidiyah M, Natsir M, Fitrianingsih F et al (2017) Lignin degradation of oil palm empty fruit bunches using TiO_2 photocatalyst as antifungal of *Fusarium oxysporum*. Orient J Chem 33:3101–3106. https://doi.org/10.13005/ojc/330651

Melkamu A, Kahsay MB, Tesfay AG (2019) Mechanical and water-absorption properties of sisal fiber (*Agave sisalana*)-reinforced polyester composite. J Nat Fibers 16:877–885. https://doi.org/10.1080/15440478.2018.1441088

Mohd Radzuan NA, Tholibon D, Sulong AB et al (2020) New processing technique for biodegradable kenaf composites: a simple alternative to commercial automotive parts. Compos Part B Eng 184:107644. https://doi.org/10.1016/j.compositesb.2019.107644

Mokbli S, Nehdi IA, Sbihi HM et al (2018) *Yucca aloifolia* seed oil: a new source of bioactive compounds. Waste Biomass Valoriz 9:1087–1093. https://doi.org/10.1007/s12649-017-9892-2

Moshi AAM, Ravindran D, Bharathi SRS et al (2020) Characterization of a new cellulosic natural fiber extracted from the root of *Ficus religiosa* tree. Int J Biol Macromol 142:212–221. https://doi.org/10.1016/j.ijbiomac.2019.09.094

Müssig J (ed) (2010) Industrial applications of natural fibres. Wiley, Chichester, UK

Nehdi IA, Sbihi HM, Mokbli S et al (2015) *Yucca aloifolia* oil methyl esters. Ind Crops Prod 69:257–262. https://doi.org/10.1016/j.indcrop.2015.02.029

Nematollahi M, Karevan M, Mosaddegh P, Farzin M (2019) Morphology, thermal and mechanical properties of extruded injection molded kenaf fiber reinforced polypropylene composites. Mater Res Express. https://doi.org/10.1088/2053-1591/ab2fbd

Noda J, Terasaki Y, Nitta Y, Goda K (2016) Tensile properties of natural fibers with variation in cross-sectional area. Adv Compos Mater 25:253–269. https://doi.org/10.1080/09243046.2014.985421

Ornaghi HL, Poletto M, Zattera AJ, Amico SC (2014) Correlation of the thermal stability and the decomposition kinetics of six different vegetal fibers. Cellulose 21:177–188. https://doi.org/10.1007/s10570-013-0094-1

Britannica, The Editors of Encyclopaedia (2015) "Agavoideae". Encyclopedia Britannica. https://www.britannica.com/plant/Agavoideae. Accessed 28 Nov 2019

Radzuan NAM, Ismail NF, Radzi MKFM et al (2019) Kenaf composites for automotive components: enhancement in machinability and moldability. Polymers (Basel) 11:1–10. https://doi.org/10.3390/polym11101707

Rajeshkumar G, Hariharan V, Sathishkumar TP (2016) Characterization of *Phoenix* sp. natural fiber as potential reinforcement of polymer composites. J Ind Text 46:667–683. https://doi.org/10.1177/1528083715591581

Ramphul H, Bhaw-Luximon A, Jhurry D (2017) Sugar-cane bagasse derived cellulose enhances performance of polylactide and polydioxanone electrospun scaffold for tissue engineering. Carbohydr Polym 178:238–250. https://doi.org/10.1016/j.carbpol.2017.09.046

Reddy KO, Ashok B, Reddy KRN et al (2014) Extraction and characterization of novel lignocellulosic fibers from *Thespesia lampas* plant. Int J Polym Anal Charact 19:48–61. https://doi.org/10.1080/1023666X.2014.854520

Rongpipi S, Ye D, Gomez ED, Gomez EW (2019) Progress and opportunities in the characterization of cellulose—an important regulator of cell wall growth and mechanics. Front Plant Sci 9:1–28. https://doi.org/10.3389/fpls.2018.01894

Schneider CA, Rasband WS, Eliceiri KW (2012) NIH image to imageJ: 25 years of image analysis. Nat Methods 9:671–675. https://doi.org/10.1038/nmeth.2089

Salit MS, Jawaid M, Bin YN, Hoque ME (eds) (2015) Manufacturing of natural fibre reinforced polymer composites. Springer International Publishing, Cham

Sanjay MR, Madhu P, Jawaid M et al (2018) Characterization and properties of natural fiber polymer composites: a comprehensive review. J Clean Prod 172:566–581. https://doi.org/10.1016/j.jclepro.2017.10.101

Sanjay MR, Siengchin S, Parameswaranpillai J et al (2019) A comprehensive review of techniques for natural fibers as reinforcement in composites: preparation, processing and characterization. Carbohydr Polym 207:108–121

Sathishkumar TP, Satheeshkumar S, Naveen J (2014) Glass fiber-reinforced polymer composites—a review. J Reinf Plast Compos 33:1258–1275. https://doi.org/10.1177/0731684414530790

Scherrer P (1912) Bestimmung der inneren Struktur und der Größe von Kolloidteilchen mittels Röntgenstrahlen BT - Kolloidchemie Ein Lehrbuch. In: Zsigmondy R (ed). Springer, Berlin, Heidelberg, pp 387–409

Segal L, Creely JJ, Martin AE, Conrad CM (1959) An empirical method for estimating the degree of crystallinity of native cellulose using the X-ray diffractometer. Text Res J 29:786–794. https://doi.org/10.1177/004051755902901003

Senthilkumar K, Saba N, Rajini N et al (2018) Mechanical properties evaluation of sisal fibre reinforced polymer composites: a review. Constr Build Mater 174:713–729. https://doi.org/10.1016/j.conbuildmat.2018.04.143

Shanmugasundaram N, Rajendran I, Ramkumar T (2018) Characterization of untreated and alkali treated new cellulosic fiber from an *Areca palm* leaf stalk as potential reinforcement in polymer composites. Carbohydr Polym 195:566–575. https://doi.org/10.1016/j.carbpol.2018.04.127

Shubhra QTH, Alam AKMM, Quaiyyum MA (2013) Mechanical properties of polypropylene composites: a review. J Thermoplast Compos Mater 26:362–391. https://doi.org/10.1177/0892705711428659

Sreenivasan VS, Rajini N, Alavudeen A, Arumugaprabu V (2015) Dynamic mechanical and thermo-gravimetric analysis of *Sansevieria cylindrica*/polyester composite: effect of fiber length, fiber loading and chemical treatment. Compos Part B Eng 69:76–86. https://doi.org/10.1016/j.compositesb.2014.09.025

Suryanto H, Marsyahyo E, Irawan YS, Soenoko R (2014) Morphology, structure, and mechanical properties of natural cellulose fiber from mendong grass (*Fimbristylis globulosa*). J Nat Fibers 11:333–351. https://doi.org/10.1080/15440478.2013.879087

Thyavihalli Girijappa YG, Mavinkere Rangappa S, Parameswaranpillai J, Siengchin S (2019) natural fibers as

sustainable and renewable resource for development of eco-friendly composites: a comprehensive review. Front Mater 6:1–14. https://doi.org/10.3389/fmats.2019.00226

Thygesen A, Oddershede J, Lilholt H et al (2005) On the determination of crystallinity and cellulose content in plant fibres. Cellulose 12:563–576. https://doi.org/10.1007/s10570-005-9001-8

Todkar SS, Patil SA (2019) Review on mechanical properties evaluation of pineapple leaf fibre (PALF) reinforced polymer composites. Compos Part B Eng 174:106927. https://doi.org/10.1016/j.compositesb.2019.106927

Van Soest PJ (1963) Use of detergents in the analysis of fibrous feeds. 2. A rapid method for the determination of fiber and lignin. J Assoc Off Agric Chem 46:829–835

Vaz S (2016) Analytical techniques and methods for biomass. Springer, Cham

Vinod A, Sanjay MR, Suchart S, Jyotishkumar P (2020) Renewable and sustainable biobased materials: an assessment on biofibers, biofilms, biopolymers and biocomposites. J Clean Prod 258:120978. https://doi.org/10.1016/j.jclepro.2020.120978

Wang F, Zhou S, Li L, Zhang X (2018) Changes in the morphological–mechanical properties and thermal stability of bamboo fibers during the processing of alkaline treatment. Polym Compos 39:E1421–E1428. https://doi.org/10.1002/pc.24332

Webber HJ (1895) Studies on the dissemination and leaf reflexion of *Yucca aloifolia* and other species. Missouri Bot Gard Annu Rep 1895:91. https://doi.org/10.2307/2992152

Yue Y, Zhou C, French AD et al (2012) Comparative properties of cellulose nano-crystals from native and mercerized cotton fibers. Cellulose 19:1173–1187. https://doi.org/10.1007/s10570-012-9714-4